ROYAL SOCIETY OF CHEMISTRY

Check for updates

Supramolecular assemblies of tetravalent terbium complex units: syntheses, structure, and materials properties†

Tianjiao Xue,[ab] Qing-Song Yang,[ab] Lei Li,[ab] Xiao-Yong Chang,[a] You-Song Ding ✱[ab] and Zhiping Zheng ✱[ab]

There is a growing interest in lanthanide complexes exhibiting unconventional oxidation states, primarily due to their unique electronic structures and accompanying physicochemical properties. Herein, likely the first examples of supramolecular assemblies of non-Ce(IV) tetravalent lanthanide complexes, with the general formula [Tb(OSiPh$_3$)$_4$Lx]$_n$ [1 ($n = 2$, L1 = 1,2-bis(4-pyridyl)ethane); 2 (L2 = 4,4′-bipyridine), 3 (L3 = 1,2-bis(4-pyridyl)acetylene), 4 (L4 = 1,2-bis(4-pyridyl)ethylene), and 5 (L5 = 1,4-bis(4-pyridyl)benzene)], are reported. Cyclic voltammetry studies show two successive redox events, indicating electronic interactions between the two Tb(IV) centers in the dimeric metallomacrocycle 1. Compounds 2–5 are zig-zag structured coordination polymers featuring complex units of Tb(OSiPh$_3$)$_4$ bridged by their respective pyridyl-based ditopic ligands. These tetravalent lanthanide species display impressive stability in air, which is believed to result from the stabilization effect of ligand Lx and the extensive multifarious interactions involving the aromatic rings of the anionic (Ph$_3$SiO$^-$) and bridging ligands. UV-vis absorption spectroscopic studies show that 2–5 are semiconducting, each with a narrow bandgap of *ca.* 1.7 eV. Magnetic property studies yielded magnetic entropy changes of *ca.* 8.0 J (kg K)$^{-1}$ at 2.5 K and 7T, which is reasonable for a complex with high-molecular-weight ligands, suggesting the potential development of Tb(IV) complexes as molecular refrigerants due to their f^7 electronic configuration.

Introduction

Complexes of metal ions in unconventional oxidation states are of fundamental scientific interest and practical significance due to their unique properties and potential materials applications.[1,2] For the lanthanide (Ln) elements, chemistry has been dominated by trivalent ions. With a few exceptions, complexes of lanthanide ions in other oxidation states, specifically divalent and tetravalent, are notoriously sensitive to air and moisture, making their synthesis challenging. For example, most Ln(II) complexes are unstable at room temperature and should be kept at low temperatures and in glove boxes.[3–39] Some Ln(II) complexes can even activate the C–H bonds (sp^3) of the ligands or solvent molecules.[7,14,18,19,25–27,34,39] However, thanks to the collective efforts of Evans, Schumann, Ziller, Protchenko, Junk, and others, complexes of all Ln(II) ions have been obtained and

structurally characterized,[4–10] some of which exhibit interesting luminescence,[12,31,40–43] magnetic,[11,22,28,32,36] or catalytic properties.[21] In comparison, the analogous research on Ln(IV) has lagged far behind, except for the well-known Ce(IV), for which some exciting new chemistry[44,45] and applications[46–52] have been reported recently.

Collectively responsible for the hiatus noted above are the scarcity of appropriate oxidants, the highly demanding synthetic procedures, and the lack of suitable ligands for the stabilization of high-valence lanthanide ions. The extreme sensitivity of such complexes to air and moisture renders their characterization and property studies difficult; there is an inherently high propensity for their decomposition in solution, including reduction by solvent molecules.[53–64] Thus so far, only a handful of Tb(IV) complexes exist and an even smaller number of complexes of Pr(IV) (Table S1†),[53–64] with only one complex of Pr(V) having being recently reported.[65]

Recently, we have made efforts to enhance the stability of complexes of Tb(IV) and Pr(IV) by replacing the coordinated solvent molecules in the benchmarking complex Tb(OSiPh$_3$)$_4$S$_2$ (S = MeCN or THF) with 1,2-dimethoxyethane (DME) and several pyridyl-based chelating ligands.[62,63] Surprisingly, the DME chelate is only marginally more stable than its THF congener, while the use of the latter group of ligands leads to markedly enhanced stability of the corresponding chelates.

^{a}Department of Chemistry, Southern University of Science and Technology, Shenzhen, Guangdong 518055, China. E-mail: dingys@sustech.edu.cn; zhengzp@sustech.edu.cn

^{b}Key Laboratory of Rare Earth Chemistry of Guangdong Higher Education Institutes, Southern University of Science and Technology, Shenzhen, Guangdong 518055, China

Experimental and computational studies indicate that the pyridyl (π)-to-Tb(IV) (5d) donation and the intramolecular π–π interactions between the aromatic rings of $OSiPh_3$ and these ancillary ligands are primarily responsible for the enhanced stability observed. These results indicate that the contribution of a ligand being merely chelating is insignificant. A corollary is that one may use almost any pyridyl-based ligand, chelating or not, to realize a great variety of Ln(IV) complexes for property studies and application exploration.

With this recognition, we set out to prepare supramolecular assemblies featuring complex units of Tb(IV) bridged by ditopic pyridyl-based ligands (**L1–L5**) and to explore the possible interactions between the individual complex units and the resulting properties. These ligands include (1,2-bis(4-pyridyl) ethane) (**L1**); 4,4′-bipyridine (**L2**); 1,2-bis(4-pyridyl)ethylene (**L3**); 1,2-bis(4-pyridyl)acetylene (**L4**), and 1,4-bis(4-pyridyl) benzene (**L5**). A straightforward replacement of MeCN in $Tb(OSiPh_3)_4(MeCN)_2$ with **Lx** affords a cyclic dimeric complex and four coordination polymers of the general formula $[Tb(OSiPh_3)_4Lx]_n$ [**1**(**L1**, $n = 2$); **2**(**L2**); **3**(**L3**), **4**(**L4**), and **5**(**L5**)]. Compounds **1–5** are likely the first polynuclear complexes of a non-Ce(IV) tetravalent lanthanide ion,[66] for which we carried out magnetic property studies originating from the f^7 electronic configuration of the Tb(IV) center.

Results and discussion

Syntheses and crystallographic studies

The title complexes were obtained by the ligand exchange reaction of $Tb(OSiPh_3)_4(MeCN)_2$ with the bridging ligands (**L1–L5**). Different from the literature synthesis, the tetravalent MeCN solvate was obtained by oxidizing the trivalent precursor complex $Tb(OSiPh_3)_3(THF)_3$ with thianthrene tetrafluoroborate in an acetonitrile solution of $KOSiPh_3$ (Scheme 1); a profound color change of the reaction mixture from pale-yellow green to orange-red was observed as the reaction progressed.[67,68] Compared with the previously used oxidant $[N(C_6H_4Br)_3]$ $[SbCl_6]$, thianthrene tetrafluoroborate offers several advantages, including its ease of synthesis and use, low cost, and straightforward isolation of the solvate product by filtration from the reduction byproduct (thianthrene).[69] All the crystals are intensely colored, with dark red for **1**, orange for **2**, and red for **3–5**. This red-orange hue is consistent with previously reported Tb(IV) complexes.[53–55,61–63]

Crystallographic studies (Table S2†) revealed the dimeric cyclic structure of **1** featuring two complex units of $Tb(OSiPh_3)_4$ bridged by two **L1** ligands (Fig. 1a). The hexacoordinate Tb atom displays a roughly octahedral coordination sphere formed by four O (Ph_3SiO^-) atoms and two pyridyl N atoms of the *cis*-disposed **L1** ligands, each adopting a *gauche–gauche* conformation to facilitate the formation of the metallomacrocycle.[70–73] With the more rigid **L2–L5**, zigzag-chain structured coordination polymers **2–5** were obtained (Fig. 1b–e). The distortion of the coordination geometry from a perfect octahedron in these polynuclear Tb(IV) complexes is estimated by continuous shape measures analysis[74] to be 0.566, 1.113–1.148, 0.849–0.940, 0.798–0.920, and 0.675 for **1–5**, respectively (Table S3†). The Tb(IV)–O bonds, ranging from 2.024(5) to 2.090(3) Å (Table S4†), are comparable to those of previously reported Tb(IV) complexes but significantly shorter than their Tb(III)-$OSiPh_3$ counterparts. The N–Tb–N angles range from 79.58(14)° to 89.4(5)° in **1–5**, which is in good agreement with previously reported Tb(IV) complexes.[53–55,61–63] The two Tb atoms in the uniquely structured **1** are separated by a distance of 10.446 Å, while the neighboring Tb atoms within the polymeric chains are separated by 12.054, 14.083, 14.207, and 16.320 Å, respectively in **2–5**, in approximate accordance with the increase in the size of the different bridging ligands.

In our recently reported Tb(IV) chelates with pyridyl-based ligands, the intramolecular π–π and C–H···π interactions between the aromatic rings of Ph_3SiO^- and the chelating ligands are believed to be critically important in improving the stability of the chelates. Similar interactions are identified in the discrete dimeric complex **1** (Fig. S1 and Table S5†).[62,63] For the coordination polymers (**2–5**), such interactions, in addition to the ones within each of the complex units, exist copiously between individual polymer chains (Fig. S2–S4†). The extensive non-covalent interactions within the complex building unit and between the polymeric chains can be appreciated from the crystal packing of **5** (Fig. 2) – a representative of the
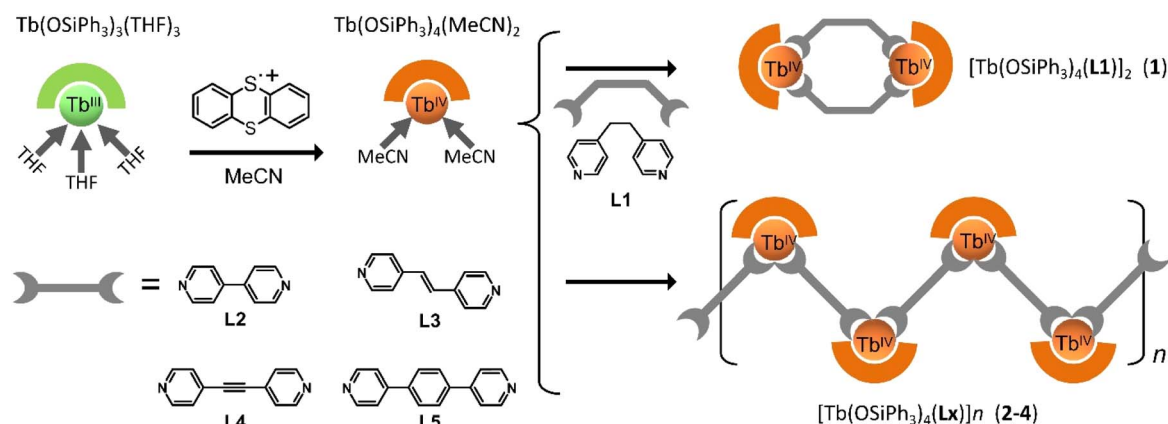
Scheme 1 The preparation of $[Tb(OSiPh_3)_4Lx]_n$ [**1** ($n = 2$), **L1** = 1,2-bis(4-pyridyl)ethane; **2**, **L2** = 4,4′-bipyridine; **3**, **L3** = 1,2-bis(4-pyridyl) acetylene; **4**, **L4** = 1,2-bis(4-pyridyl)ethylene; **5**, **L5** = 1,4-bis(4-pyridyl)benzene].
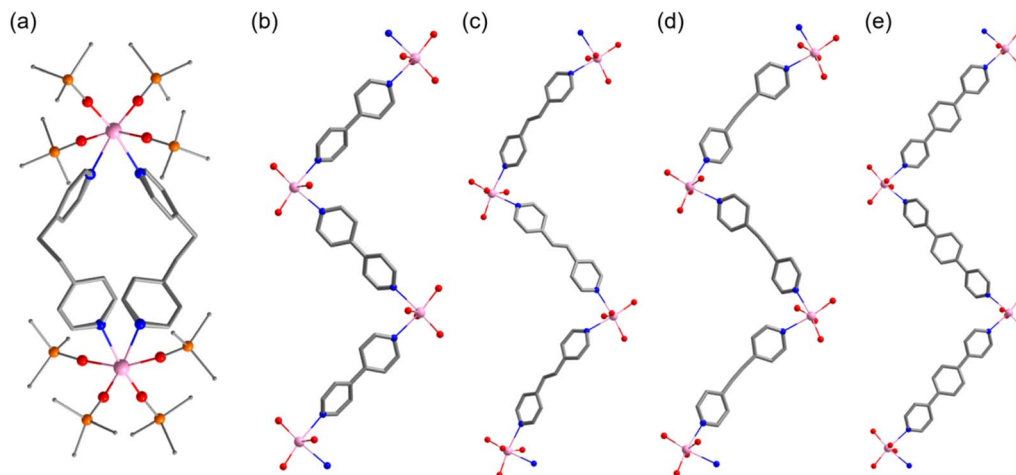
Fig. 1 The crystal structures of **1** (a), **2** (b), **3** (c), **4** (d), and **5** (e). Simplified views of the Ph$_3$SiO$^-$ ligands (O, Si, and the Si–bound C atoms in **1**, and O atoms only in **2–5**) are shown with the bridging ligands (hydrogen atoms are removed for clarity) and the Tb(IV) centers (color legends: Tb, lilac; O, red; C, grey; N, blue; Si, orange).

coordination polymers. Within the complex unit, one or two phenyl groups of the Ph$_3$SiO$^-$ ligands are disposed in such a way that strong face-to-face π–π interactions between the pyridyl ligands are present (green-colored fragments, Fig. 2). Corroborating such interactions is the pronounced deviation of the axial coordination motif from linearity (151.44(16)° to 159.03(15)°, Table S4†). Moreover, inter-chain interactions, mostly of the C–H···π type, exist amply between the Ph$_3$SiO$^-$ phenyl groups (plum-colored fragments, Fig. 2). The same type of interactions are also found between the Ph$_3$SiO$^-$ phenyl groups in one chain and the central aromatic ring of **L5** in neighboring chains (black-colored fragments, Fig. 2). The extent of such inter-chain interactions, up to 27% of the total non-covalent interactions, is verified by Hirshfeld surface analysis (Fig. S5–S26†).[75] Although individually weak, such interactions collectively contribute to the stability observed for many

supramolecular systems. For example, extensive π-interactions have been found to stabilize the organization of porphyrin and *m*-xylylene panels, affording the robust supramolecular constructs of π-Diamond.[76,77] In the present case, the extensive C–H···π interactions bring together individual polymeric chains into an intimate arrangement, resulting in significant shielding of the Tb(IV) centers and the enhanced stability observed (*vide infra*).

The four coordination polymers (**2–5**) display impressive stability when exposed to air (Fig. 3 and S27–S29†). Against the simulated pattern, the powder X-ray diffraction (PXRD) pattern of a pristine sample of **2** is shown in Fig. 3, together with the ones obtained after the sample was exposed to air for 24 and 48 hours. The solid retained its crystallinity over this extended period of air exposure, and more importantly, the recovered solids showed essentially the same PXRD patterns as the

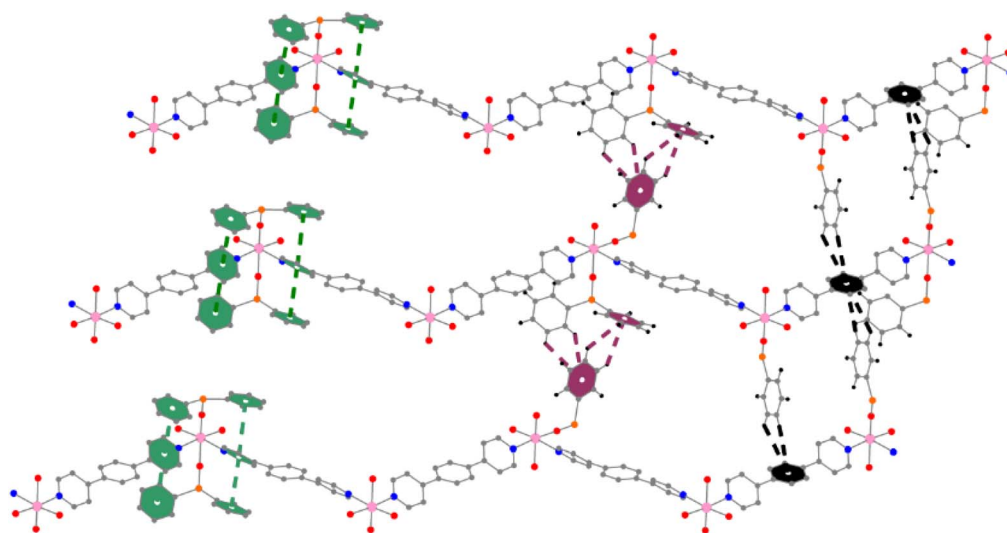**Fig. 2** Illustration of the multifarious supramolecular interaction in **5**: within any the mononuclear complex unit (green), between the Ph$_3$SiO$^-$ ligands of neighboring chains (plum), and between the Ph$_3$SiO$^-$ ligands of one chain and the bridging ligands of neighboring chains (black) (color legends: Tb, pink; O, red; Si, orange; C, gray; N, blue; H, black).
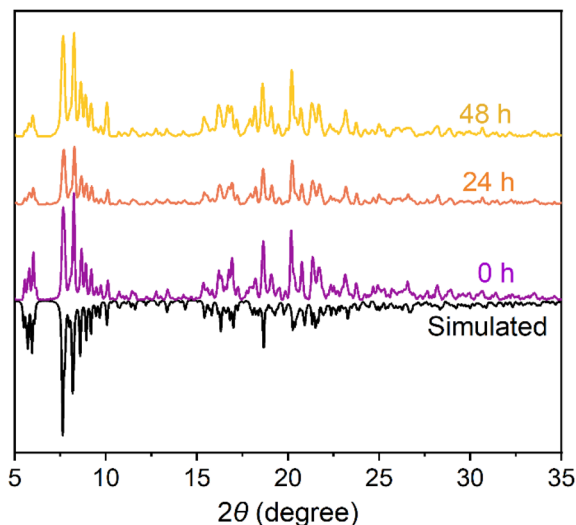
Fig. 3 Power X-ray diffraction patterns for a sample of **2** (pristine and with air exposure for 24 and 48 hours) against the one simulated based on its single-crystal structure.

pristine sample. This air-stability facilitates sample handling and any property studies of these Tb(IV) complexes.

Cyclic voltammetric study of the dimeric complex 1. Possible interactions between the two Tb(IV) centers of the dimeric complex **1** were explored using cyclic voltammetry (CV), and the results are shown in Fig. 4. Two closely spaced peaks in both oxidation and reduction were observed at different scan rates (from 50 to 1000 mV s^{-1}). The two cathodic potentials (E_{pc}), at 0.093 V and -0.255 V (at a sweep rate of 500 mV s^{-1}), indicate that **1** undergoes two successive reductions, presumably from Tb(IV)–Tb(IV) to Tb(III)–Tb(IV), and then to Tb(III)–Tb(III). The two anodic potentials (E_{pa}), at 0.344 V and 0.587 V (at a sweep rate of 500 mV s^{-1}), correspond to the stepwise re-oxidation event. As the scan rate increases, the currents of both pairs of redox peaks exhibit a similar increasing trend (Table S10†). The two
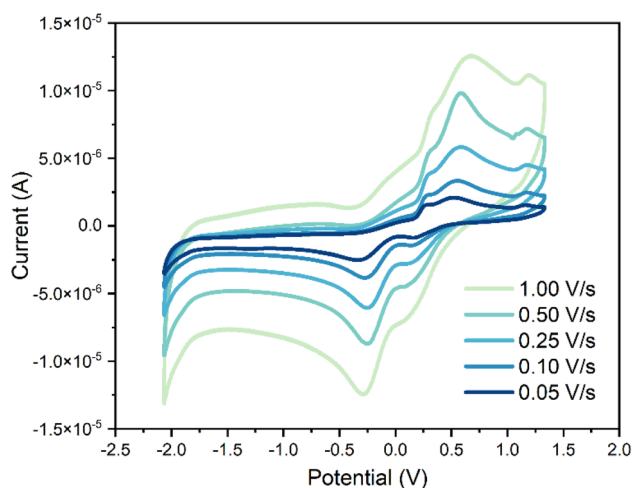

Fig. 4 Cyclic voltammograms of **1** (1.0 mM in dichloromethane) with n-Bu$_4$NPF$_6$ (0.1 mM) as the supporting electrolyte at a sweep rate of 500 mV s^{-1} versus Fc/Fc$^+$.

oxidation waves in **1** suggest the existence of weak interactions between the two Tb ions, likely occurring through space, as the two pyridyl coordinating moieties of **L1** are linked by a non-conjugated ethylene bridge. These results suggest the possibility of realizing the mixed-valence Tb(III)–Tb(IV) complex if the redox event is carefully controlled.

Physical property studies of 2–5. The properties of the insoluble polymeric complexes were investigated by solid-state ultraviolet-visible-near-infrared (UV-vis-NIR) spectroscopic studies and magnetic measurements. The broad characteristic absorption peaks (Fig. 5a), attributable to ligand-to-metal charge transitions (LMCT),[53–55,62,63] were observed between 320–650 nm (λ_{max} at 380 nm (**2**), 380 nm (**3**), 410 nm (**4**), and 395 nm (**5**)). It is worth mentioning that the absorption edges of all four polymers are at *ca.* 700 nm. The optical band gaps obtained by using the Tauc plot method based on the Kubelka–Munk theory[78] from their UV-vis-NIR spectra are between 1.66 eV and 1.70 eV (Fig. 5b), placing them within the narrow bandgap semiconductor range and suggesting potential applications in lighting and terahertz electronics. Moreover, with the paramagnetic Tb(IV) ion, spintronic applications of such magnetic semiconducting materials can also be envisioned.[79,80]

The Tb(IV) ion, with a half-filled 4f^7 electronic configuration, is isoelectronic Eu(II) and Gd(III) ions. Temperature- and field-dependent magnetic susceptibility measurements were conducted for these polymeric species. The results for the representative **3** are shown in Fig. 5c, and those for the other polymeric species are provided in Fig. S30–S32.† The χT values at 300 K are 7.90 (**2**), 7.83 (**3**), 7.84 (**4**), and 7.94 cm^3 K mol^{-1} (**5**), in good agreement with the value calculated for mononuclear 4f^7-complexes.[53–55,57,58,60–62,81] The χT value decreases slowly as the temperature is lowered to *ca.* 20 K, where a sudden drop occurs, reaching a minimum of 6.50 cm^3 K mol^{-1}. The drop in the low-temperature region is indicative of varied zero-field splitting.[60–62,81] Field-dependent magnetization measurements were subsequently performed at low temperatures with the field up to a maximum of 7T (inset in Fig. 5c for **3**). The maximum magnetization values at 2 K and 7T are 6.52 (**2**), 6.82 (**3**), 6.54 (**4**), and 6.47 μ_B (**5**), which are close to the saturation magnetization value of 7 μ_B calculated for an ion with the 4f^7 electronic configuration.[53–55,57,58,60–62,81] With the same large ground-state spin of 7/2 and magnetic isotropy as Gd(III) and Eu(II) complexes, it is entirely reasonable to explore the potential of Tb(IV) complexes as molecule-based magnetic refrigerants.[82,83] The magnetic entropy changes ($-\Delta S_m$) for the representative **3** were calculated by applying Maxwell's equation using the low-temperature field-dependent magnetization values (Fig. 5d), producing a maximum value of 8.07 J (kg K)$^{-1}$ at 2.5 K and 7T. This experimentally obtained $-\Delta S_m$ is smaller than the theoretical value of 10.15 J (kg K)$^{-1}$ ($-\Delta S_m = R\ln(2S + 1)$; R is the gas constant and S is the state spin number). Comparable magnetic entropies were obtained for the other coordination polymers, as they closely resemble **3**, both in structure and composition. However, due to the significantly higher molecular weights of the complex building unit of [Tb(OSiPh$_3$)$_4$**Lx**] (**Lx** = **L2**–**L5**),[84] the magnetocaloric effects displayed by the present Tb(IV) complexes are noticeably smaller than those of Gd(III) or Eu(II)
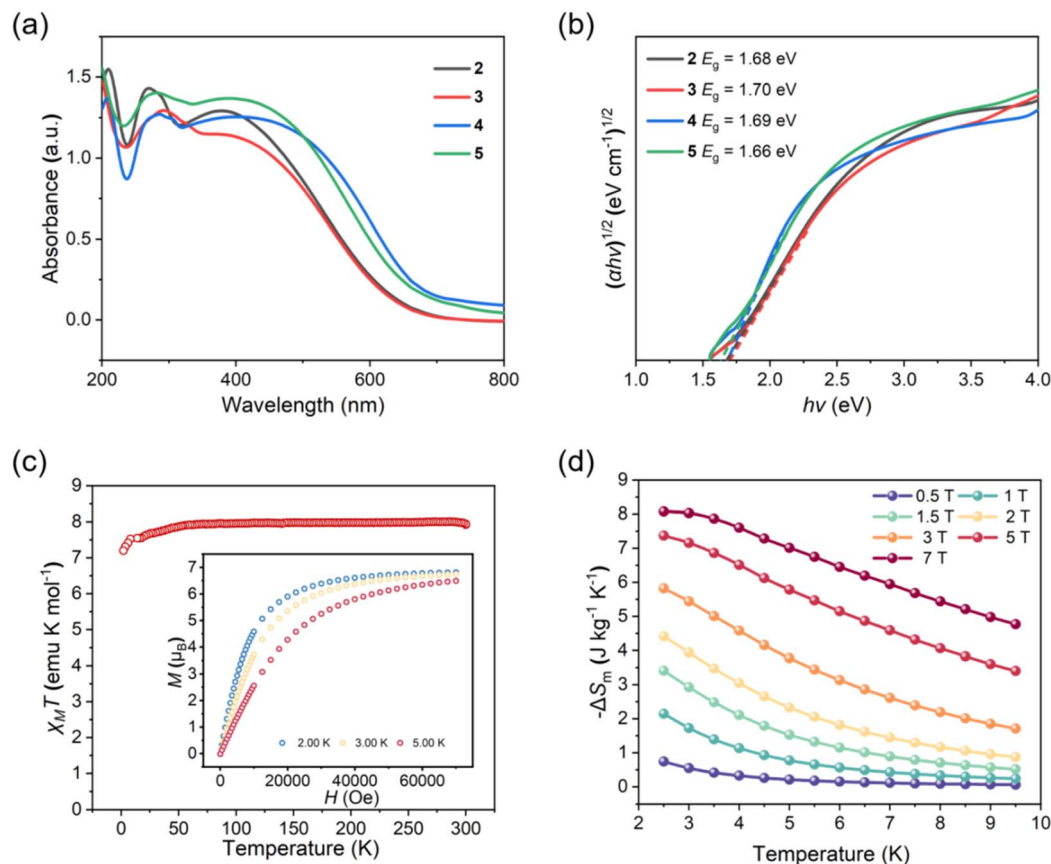
Fig. 5 Property studies of **2**–**5**. (a) Solid-state UV-vis-NIR reflectance at room temperature. (b) Determination of the optical band gaps from UV-vis-NIR spectra using the Tauc plot method at room temperature. (c) The χT versus T plot of **3** under 1000 Oe dc field (the tnset shows the field-dependent magnetization plots at 2, 3, and 5 K). (d) $-\Delta S_{\mathrm{m}}$ calculated by using the magnetization data for **3** collected at 0.5–7.0T (magnetic field) and 2.5–9.5 K (temperature).

complexes.[82,83] Possible enhancement in this regard may be achieved by increasing the mass percentage of Tb(IV) in its complexes with lower-molecular-weight ligands.

Conclusions

In this work, we report what is likely the first supramolecular assemblies composed of complex units of non-Ce(IV) tetravalent lanthanide ions. A total of four coordination polymers have been obtained with the largely rigid dipyridyl bridging ligands, while the use of a more flexible ditopic ligand afforded a dimeric metallamacrocycle. Cyclic voltammetry studies revealed significant electronic interactions between the Tb(IV) centers within the macrocycle, highlighting the rich redox chemistry enabled by uniquely structured tetravalent lanthanide complexes. The four coordination polymers survived extended air-exposure, due to a combination of the ligand stabilizing effect and the extensive intra- and inter-chain non-covalent interactions that involve the aromatic rings of both the anionic ligands in the complex unit and the bridging ligands. Physical property studies show that the coordination polymers possess optical band gaps comparable to those of some narrow bandgap semiconductors. Thanks to the f[7] electronic configuration of Tb(IV), we propose that it is possible to

design unprecedented molecule-based magnetic semi-conductors or magnetic refrigerants.

Data availability

The data supporting this article have been included as part of the ESI.†

Author contributions

TJX synthesized and characterized the compounds with the assistance of QSY and LL. TJX and XYC assisted in the X-ray crystallographic analyses. ZPZ and YSD designed the research project and directed the experiments. The manuscript was written with contributions from all authors, who have also approved the final version of the manuscript.

Conflicts of interest

There are no conflicts to declare.

Acknowledgements

Notes and references

1 J. C. Wedal and W. J. Evans, *J. Am. Chem. Soc.*, 2021, **143**, 18354–18367.

2 Y. Wang and W. Huang, *Sci. China Chem.*, 2020, **50**, 1504–1559.

3 W. J. Evans, N. T. Allen and J. W. Ziller, *J. Am. Chem. Soc.*, 2001, **123**, 7927–7928.

4 M. N. Bochkarev, I. L. Fedushkin, S. Dechert, A. A. Fagin and H. Schumann, *Angew. Chem., Int. Ed.*, 2001, **40**, 3176–3178.

5 W. J. Evans, N. T. Allen and J. W. Ziller, *Angew. Chem., Int. Ed.*, 2002, **41**, 359–361.

6 P. B. Hitchcock, M. F. Lappert, L. Maron and A. V. Protchenko, *Angew. Chem., Int. Ed.*, 2008, **47**, 1488–1491.

7 F. Jaroschik, A. Momin, F. Nief, X.-F. Le Goff, G. B. Deacon and P. C. Junk, *Angew. Chem., Int. Ed.*, 2009, **48**, 1117–1121.

8 M. R. MacDonald, J. W. Ziller and W. J. Evans, *J. Am. Chem. Soc.*, 2011, **133**, 15914–15917.

9 M. R. MacDonald, J. E. Bates, M. E. Fieser, J. W. Ziller, F. Furche and W. J. Evans, *J. Am. Chem. Soc.*, 2012, **134**, 8420–8423.

10 M. R. MacDonald, J. E. Bates, J. W. Ziller, F. Furche and W. J. Evans, *J. Am. Chem. Soc.*, 2013, **135**, 9857–9868.

11 K. R. Meihaus, M. E. Fieser, J. F. Corbey, W. J. Evans and J. R. Long, *J. Am. Chem. Soc.*, 2015, **137**, 9855–9860.

12 A. N. W. Kuda-Wedagedara, C. Wang, P. D. Martin and M. J. Allen, *J. Am. Chem. Soc.*, 2015, **137**, 4960–4963.

13 M. E. Fieser, M. R. MacDonald, B. T. Krull, J. E. Bates, J. W. Ziller, F. Furche and W. J. Evans, *J. Am. Chem. Soc.*, 2015, **137**, 369–382.

14 J. F. Corbey, D. H. Woen, C. T. Palumbo, M. E. Fieser, J. W. Ziller, F. Furche and W. J. Evans, *Organometallics*, 2015, **34**, 3909–3921.

15 L. A. Ekanger, D. R. Mills, M. M. Ali, L. A. Polin, Y. Shen, E. M. Haacke and M. J. Allen, *Inorg. Chem.*, 2016, **55**, 9981–9988.

16 M. Xémard, A. Jaoul, M. Cordier, F. Molton, O. Cador, B. Le Guennic, C. Duboc, O. Maury, C. Clavaguéra and G. Nocton, *Angew. Chem., Int. Ed.*, 2017, **56**, 4266–4271.

17 R. P. Kelly, L. Maron, R. Scopelliti and M. Mazzanti, *Angew. Chem., Int. Ed.*, 2017, **56**, 15663–15666.

18 M. E. Fieser, C. T. Palumbo, H. S. La Pierre, D. P. Halter, V. K. Voora, J. W. Ziller, F. Furche, K. Meyer and W. J. Evans, *Chem. Sci.*, 2017, **8**, 7424–7433.

19 C. T. Palumbo, D. P. Halter, V. K. Voora, G. P. Chen, J. W. Ziller, M. Gembicky, A. L. Rheingold, F. Furche, K. Meyer and W. J. Evans, *Inorg. Chem.*, 2018, **57**, 12876–12884.

20 D. P. Halter, C. T. Palumbo, J. W. Ziller, M. Gembicky, A. L. Rheingold, W. J. Evans and K. Meyer, *J. Am. Chem. Soc.*, 2018, **140**, 2587–2594.

21 F. D. White, C. Celis-Barros, J. Rankin, E. Solís-Céspedes, D. Dan, A. N. Gaiser, Y. Zhou, J. Colangelo, D. Páez-Hernández, R. Arratia-Pérez and T. E. Albrecht-Schmitt, *Inorg. Chem.*, 2019, **58**, 3457–3465.

22 C. A. Gould, K. R. McClain, J. M. Yu, T. J. Groshens, F. Furche, B. G. Harvey and J. R. Long, *J. Am. Chem. Soc.*, 2019, **141**, 12967–12973.

23 D. N. Huh, S. R. Ciccone, S. Bekoe, S. Roy, J. W. Ziller, F. Furche and W. J. Evans, *Angew. Chem., Int. Ed.*, 2020, **59**, 16141–16146.

24 S. A. Moehring, M. Miehlich, C. J. Hoerger, K. Meyer, J. W. Ziller and W. J. Evans, *Inorg. Chem.*, 2020, **59**, 3207–3214.

25 A. J. Ryan, J. W. Ziller and W. J. Evans, *Chem. Sci.*, 2020, **11**, 2006–2014.

26 T. F. Jenkins, S. Bekoe, J. W. Ziller, F. Furche and W. J. Evans, *Organometallics*, 2021, **40**, 3917–3925.

27 A. B. Chung, A. J. Ryan, M. Fang, J. W. Ziller and W. J. Evans, *Inorg. Chem.*, 2021, **60**, 15635–15645.

28 J. Moutet, J. Schleinitz, L. La Droitte, M. Tricoire, F. Pointillart, F. Gendron, T. Simler, C. Clavaguéra, B. Le Guennic, O. Cador and G. Nocton, *Angew. Chem., Int. Ed.*, 2021, **60**, 6042–6046.

29 D. N. Huh, J. P. Bruce, S. Ganesh Balasubramani, S. R. Ciccone, F. Furche, J. C. Hemminger and W. J. Evans, *J. Am. Chem. Soc.*, 2021, **143**, 16610–16620.

30 A. B. Chung, D. Rappoport, J. W. Ziller, R. E. Cramer, F. Furche and W. J. Evans, *J. Am. Chem. Soc.*, 2022, **144**, 17064–17074.

31 R. M. Diaz-Rodriguez, D. A. Gálico, D. Chartrand, E. A. Suturina and M. Murugesu, *J. Am. Chem. Soc.*, 2022, **144**, 912–921.

32 K. Kundu, J. R. K. White, S. A. Moehring, J. M. Yu, J. W. Ziller, F. Furche, W. J. Evans and S. Hill, *Nat. Chem.*, 2022, **14**, 392–397.

33 L. M. Anderson-Sanchez, J. M. Yu, J. W. Ziller, F. Furche and W. J. Evans, *Inorg. Chem.*, 2023, **62**, 706–714.

34 C. R. Stennett, J. Q. Nguyen, J. W. Ziller and W. J. Evans, *Organometallics*, 2023, **42**, 696–707.

35 W. N. G. Moore, T. J. McSorley, A. Vincent, J. W. Ziller, L. A. Jauregui and W. J. Evans, *ACS Appl. Nano Mater.*, 2023, **6**, 6461–6466.

36 P.-B. Jin, Q.-C. Luo, G. K. Gransbury, I. J. Vitorica-Yrezabal, T. Hajdu, I. Strashnov, E. J. L. McInnes, R. E. P. Winpenny, N. F. Chilton, D. P. Mills and Y.-Z. Zheng, *J. Am. Chem. Soc.*, 2023, **145**, 27993–28009.

37 P. W. Smith, J. Hrubý, W. J. Evans, S. Hill and S. G. Minasian, *J. Am. Chem. Soc.*, 2024, **146**, 5781–5785.

38 D. Errulat, K. L. M. Harriman, D. A. Gálico, E. V. Salerno, J. van Tol, A. Mansikkamäki, M. Rouzières, S. Hill, R. Clérac and M. Murugesu, *Nat. Commun.*, 2024, **15**, 3010.

39 J. D. Queen, L. M. Anderson-Sanchez, C. R. Stennett, A. Rajabi, J. W. Ziller, F. Furche and W. J. Evans, *J. Am. Chem. Soc.*, 2024, **146**, 3279–3292.

40 G. Zhan, L. Wang, Z. Zhao, P. Fang, Z. Bian and Z. Liu, *Angew. Chem., Int. Ed.*, 2020, **59**, 19011–19015.

41 W. Yan, T. Li, Z. Cai, H. Qi, R. Guo, P. Huo, Z. Liu and Z. Bian, *Inorg. Chem. Front.*, 2022, **9**, 4794–4800.

42 W. Yan, Z. Zhao, G. Yu, H. Qi, R. Guo, N. Zheng, Z. Bian and Z. Liu, *Sci. China Chem.*, 2023, **66**, 1750–1757.

43 R. M. Diaz-Rodriguez, D. A. Gálico, D. Chartrand and M. Murugesu, *J. Am. Chem. Soc.*, 2024, **146**, 34118–34129.

44 Y. Wang, J. Liang, C. Deng, R. Sun, P.-X. Fu, B.-W. Wang, S. Gao and W. Huang, *J. Am. Chem. Soc.*, 2023, **145**, 22466–22474.

45 Y. Guo, X.-L. Jiang, Q.-Y. Wu, K. Liu, W. Wang, K.-Q. Hu, L. Mei, Z.-F. Chai, J. K. Gibson, J.-P. Yu, J. Li and W.-Q. Shi, *J. Am. Chem. Soc.*, 2024, **146**, 7088–7096.

46 Y. Qiao and E. J. Schelter, *Acc. Chem. Res.*, 2018, **51**, 2926–2936.

47 A. Hu, J.-J. Guo, H. Pan and Z. Zuo, *Science*, 2018, **361**, 668–672.

48 Q. Yang, Y.-H. Wang, Y. Qiao, M. Gau, P. J. Carroll, P. J. Walsh and E. J. Schelter, *Science*, 2021, **372**, 847–852.

49 G. B. Panetti, D.-C. Sergentu, M. R. Gau, P. J. Carroll, J. Autschbach, P. J. Walsh and E. J. Schelter, *Nat. Commun.*, 2021, **12**, 1713.

50 Q. An, Y.-Y. Xing, R. Pu, M. Jia, Y. Chen, A. Hu, S.-Q. Zhang, N. Yu, J. Du, Y. Zhang, J. Chen, W. Liu, X. Hong and Z. Zuo, *J. Am. Chem. Soc.*, 2023, **145**, 359–376.

51 H. Tateyama, A. C. Boggiano, C. Liao, K. S. Otte, X. Li and H. S. La Pierre, *J. Am. Chem. Soc.*, 2024, **146**, 10268–10273.

52 Q. An, L. Chang, H. Pan and Z. Zuo, *Acc. Chem. Res.*, 2024, **57**, 2915–2927.

53 C. T. Palumbo, I. Zivkovic, R. Scopelliti and M. Mazzanti, *J. Am. Chem. Soc.*, 2019, **141**, 9827–9831.

54 A. R. Willauer, C. T. Palumbo, R. Scopelliti, I. Zivkovic, I. Douair, L. Maron and M. Mazzanti, *Angew. Chem., Int. Ed.*, 2020, **59**, 3549–3553.

55 A. R. Willauer, I. Douair, A.-S. Chauvin, F. Fadaei-Tirani, J.-C. G. Bünzli, L. Maron and M. Mazzanti, *Chem. Sci.*, 2022, **13**, 681–691.

56 A. R. Willauer, C. T. Palumbo, F. Fadaei-Tirani, I. Zivkovic, I. Douair, L. Maron and M. Mazzanti, *J. Am. Chem. Soc.*, 2020, **142**, 5538–5542.

57 N. T. Rice, I. A. Popov, D. R. Russo, J. Bacsa, E. R. Batista, P. Yang, J. Telser and H. S. La Pierre, *J. Am. Chem. Soc.*, 2019, **141**, 13222–13233.

58 N. T. Rice, I. A. Popov, D. R. Russo, T. P. Gompa, A. Ramanathan, J. Bacsa, E. R. Batista, P. Yang and H. S. La Pierre, *Chem. Sci.*, 2020, **11**, 6149–6159.

59 N. T. Rice, I. A. Popov, R. K. Carlson, S. M. Greer, A. C. Boggiano, B. W. Stein, J. Bacsa, E. R. Batista, P. Yang and H. S. La Pierre, *Dalton Trans.*, 2022, **51**, 6696–6706.

60 T. P. Gompa, S. M. Greer, N. T. Rice, N. Jiang, J. Telser, A. Ozarowski, B. W. Stein and H. S. La Pierre, *Inorg. Chem.*, 2021, **60**, 9064–9073.

61 M. Tricoire, F.-C. Hsueh, M. Keener, T. Rajeshkumar, R. Scopelliti, I. Zivkovic, L. Maron and M. Mazzanti, *Chem. Sci.*, 2024, **15**, 6874–6883.

62 T. Xue, Y.-S. Ding, X.-L. Jiang, L. Tao, J. Li and Z. Zheng, *Precis. Chem.*, 2023, **1**, 583–591.

63 T. Xue, Y.-S. Ding and Z. Zheng, *Dalton Trans.*, 2024, **53**, 5779–5783.

64 A. C. Boggiano, S. R. Chowdhury, M. D. Roy, M. G. Bernbeck, S. M. Greer, B. Vlaisavljevich and H. S. La Pierre, *Angew. Chem., Int. Ed.*, 2024, **63**, e202409789.

65 A. Boggiano, C. Studvick, S. Roy Chowdhury, J. Niklas, H. Tateyama, H. Wu, *et al.*, Praseodymium in the Formal +5 Oxidation State, *ChemRxiv*, 2024, preprint, DOI: **10.26434/chemrxiv-2024-cb3zj**, This content is a preprint and has not been peer-reviewed.

66 Z. Guo, G. B. Deacon and P. C. Junk, *J. Coord. Chem.*, 2024, 1–6.

67 M. J. McGeary, P. S. Coan, K. Folting, W. E. Streib and K. G. Caulton, *Inorg. Chem.*, 1991, **30**, 1723–1735.

68 B. Boduszek and H. J. Shine, *J. Org. Chem.*, 1988, **53**, 5142–5143.

69 N. G. Connelly and W. E. Geiger, *Chem. Rev.*, 1996, **96**, 877–910.

70 W.-H. Zhang, Y.-L. Song, Z.-H. Wei, L.-L. Li, Y.-J. Huang, Y. Zhang and J.-P. Lang, *Inorg. Chem.*, 2008, **47**, 5332–5346.

71 V. Chandrasekhar, T. Hajra, J. K. Bera, S. M. W. Rahaman, N. Satumtira, O. Elbjeirami and M. A. Omary, *Inorg. Chem.*, 2012, **51**, 1319–1329.

72 W. Zheng, S.-T. Jiang, B. Jiang and H.-B. Yang, in *Metallomacrocycles: From Structures to Applications*, ed. H.-B. Yang, The Royal Society of Chemistry, 2018, pp. 1–19, DOI: **10.1039/9781788013123-00001**.

73 G. J. Douglas, E. Richards and S. Sproules, *Chem. Commun.*, 2025, **61**, 685–688.

74 S. Alvarez, D. Avnir, M. Llunell and M. Pinsky, *New J. Chem.*, 2002, **26**, 996–1009.

75 P. R. Spackman, M. J. Turner, J. J. McKinnon, S. K. Wolff, D. J. Grimwood, D. Jayatilaka and M. A. Spackman, *J. Appl. Crystallogr.*, 2021, **54**, 1006–1011.

76 K. Liang, Y. Liang, M. Tang, J. Liu, Z.-B. Tang and Z. Liu, *Angew. Chem., Int. Ed.*, 2024, **63**, e202409507.

77 P. Harding and D. J. Harding, *Trends Chem.*, 2024, **6**, 575–576.

78 P. Makuła, M. Pacia and W. Macyk, *J. Phys. Chem. Lett.*, 2018, **9**, 6814–6817.

79 Y. H. Lee, *Science*, 2023, **382**, eadl0823.

80 L. Li, Y.-S. Ding and Z. Zheng, *Angew. Chem., Int. Ed.*, 2024, **63**, e202410019.

81 J. B. Petersen, Y.-S. Ding, S. Gupta, A. Borah, E. J. L. McInnes, Y.-Z. Zheng, R. Murugavel and R. E. P. Winpenny, *Inorg. Chem.*, 2023, **62**, 8435–8441.

82 B. Wang, X. Liu, F. Hu, J.-t. Wang, J. Xiang, P. Sun, J. Wang, J. Sun, T. Zhao, Z. Mo, J. Shen, Y. Chen, Q. Huang and B. Shen, *J. Am. Chem. Soc.*, 2024, **146**, 35016–35022.

83 Q. Xu, B. Liu, M. Ye, G. Zhuang, L. Long and L. Zheng, *J. Am. Chem. Soc.*, 2022, **144**, 13787–13793.

84 Y.-S. Ding and Y.-Z. Zheng, *J. Rare Earths*, 2021, **39**, 1554–1559.